Controlling the Sense of Agency in Dyadic Robot Interaction: An Active Inference Approach

Nadine Wirkuttis[1] and Jun Tani[2,*]

***Abstract*— This study investigated how social interaction among robotic agents changes dynamically depending on individual sense of agency. In a set of simulation studies, we examine dyadic imitative interactions of robots using a variational recurrent neural network model. The model is based on the free energy principle such that interacting robots find themselves in a loop, attempting to predict and infer each other's actions using active inference. We examined how regulating the complexity term to minimize free energy during training determines the dynamic characteristics of networks and affects dyadic imitative interactions. Our simulation results show that through softer regulation of the complexity term, a robot with stronger agency develops and dominates its counterpart developed with weaker agency through tighter regulation. When two robots are trained with equally soft regulation, both generate individual intended behavior patterns, ignoring each other. We argue that primary intersubjectivity does develop in dyadic robotic interactions.**

I. Introduction

Social interaction is considered an essential cognitive behavior in robots as well as in humans. In both empirical studies and synthetic modeling, researchers have investigated underlying cognitive, psychological, or neuronal mechanisms accounting for various aspects of social cognitive behaviors. The current study investigates mechanisms underlying synchronized imitation as a representative social cognitive act, by conducting simulation experiments on dyadic interaction between robots. In particular, we examined how a sense of agency (SoA) [1] develops in each robot during learning and how it affects synchronized imitative interactions between robots. Here, SoA denotes a specific feeling that "I am the one generating this action", which refers more formally to congruence between an agent's intention or belief in an action and its anticipated outcome.

Numerous robotic studies have investigated imitative interaction. In the 90s, imitation was identified as an indispensable human competency required in early development of cognitive behaviors [2], [3], [4], [5], [6]. Rizzolatti and colleagues [7] showed that the mirror neuron system (MNS) uses observations of an action to generate the same action. Arbib and Oztop [8], [9] indicated that mirror neurons may participate in imitative behaviors. Upon this development, several research groups proposed mirror neuron-related models for imitation using hidden Markov models [10], neural network models [11], [12], [13], [14], [15], and combinations for computational models resembling staged cognitive development [16].

A logical question is, "How can the agency of an agent, robot or human, be exerted if imitation elicited by an MNS mechanism serves as the default mode?" [17]. Sometimes agents generate their own intended actions, regardless of movements demonstrated by others, while in other cases, they imitate and follow actions of others.

Recent theories on predictive coding (PC) and active inference (AIF) based on the free energy principle (FEP) developed by Friston and others [18], [19] show that intention, i.e., belief of an agent, can be formulated as a predictive model. Furthermore, they showed that congruence between predicted action outcomes and observations reinforce the SoA [20].

On a related topic, Ahmadi and Tani developed predictive-coding inspired variational RNN (PV-RNN) [21]. Their model was used to investigate how the strength of top-down intention in predicting fluctuating temporal patterns was modulated, depending on learning conditions in the model. In the learning process, free energy represented by the weighted sum of the accuracy term and the complexity term is minimized. Ahmadi and Tani found that softer regulation of the complexity term during network training develops strong top-down intention. Predictions are more deterministic by self-organizing deterministic dynamics with the initial sensitivity characteristics in the model network. Likewise, tighter regulation of the complexity term results in weaker intention and increased stochasticity.

Compared to other neural network models based on the FEP [22], [23], [24], [25], PV-RNN has advantages when applied to problems in robotics. It can cope with temporal structure by using the recurrence associated with stochastic latent variables and by hierarchical abstraction through a multiple timescale structure [26].

Our research group investigated human-robot imitative interaction, focusing on agency using PV-RNN. Chame and Tani [27] showed that a humanoid robot with force feedback control tends to lead or follow the human counterpart in imitative interaction using haptics when its PV-RNN is set with looser or tighter regulation, respectively. Ohata and Tani [17] investigated imitative interaction between a robot and a human via visuo-proprioceptive sensation. They showed that the same tendency as in [27] can be observed even when regulation of the complexity term is modulated during the interaction phase, rather than during the prior learning phase. These synthetic experiments support a hypothesis that primary intersubjectivity [28] is a "non-mentalist, pre-

This work was sponsored by the Okinawa Institute of Science and Technology Graduate University, Okinawa, Japan 904-0302.

[1] The authors are with the Cognitive Neurorobotics Research Unit, Okinawa Institute of Science and Technology Graduate University, Okinawa, Japan 904-0302. {nadine.wirkuttis, jun.tani}@oist.jp

*Corresponding author.

theoretical, non-conceptual sort of process that grounds a certain level of communication and understanding" [27], developed in the dense interaction dynamics instantiated by active inference.

The main contribution of the current study is to clarify the underlying mechanism of dyadic synchronized imitative interaction related to the sense of agency of each individual by conducting synthetic studies using two robots. The interaction experiment considers two robotic agents that are trained to generate a set of movement primitive sequences. Those are generated by following a probabilistic finite state machine (P-FSM), the transition probability of which differs, depending partially on each of the two robots. After each robot learns the given probabilistic transition structure for a sequence, the experimental design allows us to investigate how two robots generate movement primitives in the synchronised imitative interaction setting. In particular, it should be interesting to examine conflicting situations wherein each robot prefers to generate different movement patterns, depending on its own learned experience. Do they synchronize to generate the same movement pattern with one robot following the other by adapting its intention? Or do they desynchronize by generating different movement patterns, ignoring their counterparts by following their own intentions? The current study hypothesizes that whether they synchronise or desynchronize should depend on the relative strength of the SoA between the robots.

II. Model

A. Predictive Coding and Active Inference

The current study applies the concepts of PC and AIF based on FEP [18]. PC considers perception as the interplay between *a prior* expectation of a sensation and a posterior inference about a sensory outcome. Expectation of the sensation can be modeled by a generative model that maps the prior of the latent state to the expectation of sensation. The posterior inference of the observed sensation can be achieved by computing the error between the expected sensation and its outcome. This is achieved by jointly minimizing the Kullback-Leibler (KL) divergence between the posterior and the prior distributions. Both, the prior and the posterior are represented by Gaussian probability distributions using means and variances. This minimization is achieved by summation of two terms, *accuracy* and *complexity* and may be viewed as minimizing the free energy or maximizing the lower bound of the logarithm of marginal likelihood.

$$\ln p_\theta(\boldsymbol{X}) \geq \underbrace{\int q_\phi(\boldsymbol{z}|\boldsymbol{X}) \ln \frac{p_\theta(\boldsymbol{X},\boldsymbol{z})}{q_\phi(\boldsymbol{z}|\boldsymbol{X})} d\boldsymbol{z}}_{\text{Evidence lower bound}} = \underbrace{\mathbb{E}_{q_\phi(\boldsymbol{z}|\boldsymbol{X})}[\ln p_\theta(\boldsymbol{X}|\boldsymbol{z})]}_{\text{Accuracy}} - \underbrace{D_{\mathrm{KL}}[q_\phi(\boldsymbol{z}|\boldsymbol{X})\|p(\boldsymbol{z})]}_{\text{Complexity}} \tag{1}$$

$\boldsymbol{z}$, $\boldsymbol{X}$, and $q_\phi(\boldsymbol{z}|\boldsymbol{X})$ denote the latent state, the observation, and the approximate posterior, respectively. θ and ϕ are the parameters of the model. In maximizing the lower bound, the interplay between *accuracy* and *complexity* characterizes the model performance in learning, prediction, and inference.

Consistent with the AIF, actions are generated so that the error between the expected sensory outcome and the actual outcome is minimized. In robotic applications, this is equivalent to determining how expected proprioception can be achieved by generating adequate motor torque using appropriate robot joint angles. A simple solution is to use a PID controller, by which adequate motor torque to minimize errors between expected joint angles and actual angles can be obtained by means of error feedback schemes. Finally, perception by predictive coding and action generation active inference are deployed, simultaneously, closing the gap between action and perception.

B. Overview of PV-RNN

The PV-RNN model is designed to predict future sensation by means of prior generation, while reflecting the past by means of posterior inference (see Fig. 1). It also employs multiple timescales [26] to support development of hierarchical information processing. The following briefly describes the two essential parts, a *generative model* which is used for prior generation to make future predictions, and an *inference model*, which is used for posterior inference about the past. For further details, see [21], [17].

1) Generative Model: The stochastic generative model is used for prior generation, as illustrated in the future prediction part (after time step 4 in Fig. 1). PV-RNN is comprised

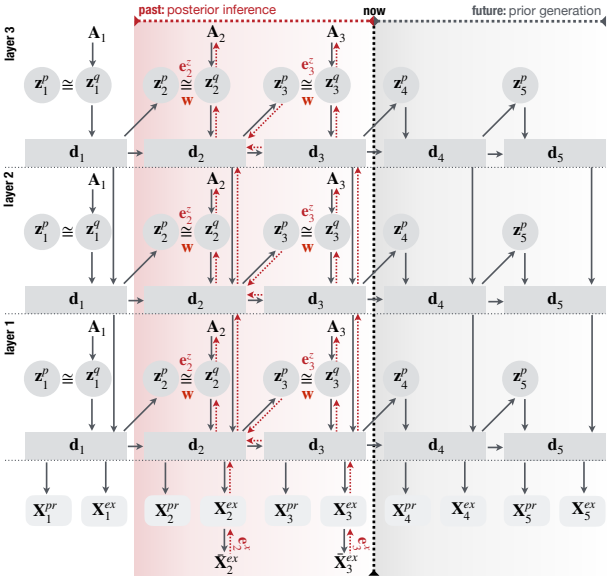

Fig. 1: **Graphical representation of a hierarchical 3-layer PV-RNN architecture.** The representation shows the network in $t = 3$ with a two-time-step posterior inference window $[2, 3]$ and prior generation for $t = [4, 5]$.

of deterministic variables $\mathbf{d}$ and stochastic variables $\mathbf{z}$. An approximate posterior distribution q is inferred based on the prior distribution p by means of error minimization on the generated output $\mathbf{X}$. The generative model parameterized

with p_θ can be factorized as shown in Eq. (2).

$$p_\theta(\boldsymbol{x}_{1:T}, \boldsymbol{d}_{1:T}, \boldsymbol{z}_{1:T}|\boldsymbol{d}_0) = \prod_{t=1}^{T} p_{\theta_x}(\boldsymbol{x}_t|\boldsymbol{d}_t) p_{\theta_d}(\boldsymbol{d}_t|\boldsymbol{d}_{t-1}, \boldsymbol{z}_t) p_{\theta_z}(\boldsymbol{z}_t|\boldsymbol{d}_{t-1}) \tag{2}$$

Note that $\boldsymbol{x}$ is conditioned directly on $\boldsymbol{z}$ through $\boldsymbol{d}$, which is a Dirac delta function.

$$\boldsymbol{d}_t = \begin{cases} 0 & \text{if } t = 0 \\ f_{\theta_d}(\boldsymbol{d}_{t-1}, \boldsymbol{z}_t) & \text{if } t > 0 \end{cases} \tag{3}$$

f_{θ_d} is a dynamic function and $\boldsymbol{d}$ is the output of the network, which internal state before activation is denoted by $\boldsymbol{h}$. This internal state $\boldsymbol{h}$ is calculated as the sum of the latent random variable $\boldsymbol{z}$, and the outputs of the current level l and the next higher level $l+1$ in the previous step, as shown in Eq. (4).

$$\begin{aligned} \boldsymbol{d}_t^l &= \tanh(\boldsymbol{h}_t^l) \\ \boldsymbol{h}_t^l &= \left(1 - \frac{1}{\tau^l}\right) \boldsymbol{h}_{t-1}^l \\ &\quad + \frac{1}{\tau^l} \left(\boldsymbol{W}_{d,d}^{l,l} \boldsymbol{d}_{t-1}^l + \boldsymbol{W}_{z,d}^{l,l} \boldsymbol{z}_t^l + \boldsymbol{W}_{d,d}^{l+1,l} \boldsymbol{d}_{t-1}^{l+1} \right) \end{aligned} \tag{4}$$

$\boldsymbol{W}$ represent connectivity weight matrices between layers and their deterministic and stochastic units.

The prior distribution $p(\boldsymbol{z}_t)$ is a Gaussian distribution represented with mean $\boldsymbol{\mu}_t^p$ and standard deviation $\boldsymbol{\sigma}_t^p$. The prior depends on $\boldsymbol{d}_{t-1}$ by following the idea of a sequence prior [29], except at t_0 where it follows a unit Gaussian distribution.

$$\begin{aligned} p(\boldsymbol{z}_1) &= \mathcal{N}(0, I) \\ p(\boldsymbol{z}_t|\boldsymbol{d}_{t-1}) &= \mathcal{N}(\boldsymbol{\mu}_t^p, (\boldsymbol{\sigma}_t^p)^2) \text{ where } t > 1 \\ \boldsymbol{\mu}_t^p &= \tanh(\boldsymbol{W}_{d,z,\mu^p}^{l,l} \boldsymbol{d}_{t-1}) \\ \boldsymbol{\sigma}_t^p &= \exp(\boldsymbol{W}_{d,z,\sigma^p}^{l,l} \boldsymbol{d}_{t-1}) \end{aligned} \tag{5}$$

2) Inference Model: Like the prior p, the posterior q is also a Gaussian distribution with mean $\boldsymbol{\mu}_t^q$ and standard deviation $\boldsymbol{\sigma}_t^q$. Since computing the true posterior is intractable, an approximate posterior $q(\boldsymbol{z})$ is inferred by maximizing the lower bound shown in Eq. (1). This inference is performed during learning and afterward, during action and perception. Fig. 1 illustrates the information flow in the posterior inference in a time window from time step 2 to time step 3.

Let us consider the posterior inference with a given sensory observation $\overline{X}_{0:T}$ for a time window from time step $t = 1$ to T. The inference model Q_ϕ for the approximate posterior is defined with the parameters ϕ as:

$$Q_\phi(\boldsymbol{z}_t|\boldsymbol{d}_{t-1}, \boldsymbol{e}_{t:T}) = \mathcal{N}(\boldsymbol{z}_t; \boldsymbol{\mu}_t^q, \boldsymbol{\sigma}_t^q) \tag{6}$$

where $\boldsymbol{e}_t^x$ denotes the error between the target $\bar{\mathbf{X}}_t$ and the predicted output $\mathbf{X}_t$. The approximate posterior for $\boldsymbol{z}_{0:T}$ is derived by:

$$\begin{aligned} q(\boldsymbol{z}_t|\boldsymbol{e}_{t:T}^x) &= \mathcal{N}(\boldsymbol{\mu}_t^q, \boldsymbol{\sigma}_t^q) \\ \boldsymbol{\mu}_t^q &= \tanh(\boldsymbol{A}_t^\mu) \\ \boldsymbol{\sigma}_t^q &= \exp(\boldsymbol{A}_t^\sigma) \end{aligned} \tag{7}$$

The adaptation variable $\mathbf{A}_{0:T}$ represents the parameters ϕ for the inference model Q_ϕ which can be optimized by maximizing the lower bound, analogous to Eq. (1),

$$p_\theta(\boldsymbol{x}_{1:T}|\boldsymbol{d}_{t0-1}) \geq L(\theta, \phi, \theta) \tag{8}$$

Then, the lower bound of PV-RNN can be derived as:

$$\begin{aligned} L(\theta, \phi, \theta) = \sum_{t=0}^{T} \Big(& \frac{1}{N_x} E_{q_\phi(\boldsymbol{z}_t|\boldsymbol{z}_{1:t-1}, \boldsymbol{e}_{t:T})} [\log p_{\theta_x}(\boldsymbol{x}_t|\tilde{\boldsymbol{d}}_t)] \\ & - \sum_{l}^{L} \frac{\mathbf{w}^l}{N_{z,l}} D_{KL}[q_\phi(\boldsymbol{z}_t|\boldsymbol{e}_{t:T}) || p_{\theta_z}(\boldsymbol{z}_t|\tilde{\boldsymbol{d}}_{t-1})] \Big) \end{aligned} \tag{9}$$

where the first term is the accuracy and the second term is the complexity (for details referred to [21]). N_x and $N_{z,l}$ are the number of sensory dimensions and the number of the latent random variables at the l^{th} layer, respectively. $\mathbf{w}^l$ is referred to as the meta-prior [21], which works as a weighting parameter for the complexity term in layer l. Networks were trained with hierarchically increasing meta-priors $\mathbf{w}$ as well as increasing time constants τ. That way, we can impose a hierarchy on the complexity term, i.e. precision, for each layer. In particular, the lower layer precision encodes a short term, sensory precision, whereas the higher layers can be considered as long term, belief precision. Note, the prior $p_{\theta_z}(\mathbf{z}_1)$ is set as a unit Gaussian with $\boldsymbol{\sigma}_t^{p,l} = 0.0$ and $\boldsymbol{\mu}_t^{p,l} = 1.0$ in $t = 1$. Note that $\mathbf{w}_1^l$ is set with 1.0[1], whereas $\mathbf{w}_{2:T}^l$ is set to a specific value when the sequence prior [29] is used after time step 1.

By setting $\mathbf{w}$ to a value ≤ 1, the complexity term imposes a unit Gaussian prior to the sequential prior and stochastic network behavior can be expected. With increasing $\mathbf{w}$, also considered as looser regulation of the complexity term, the network develops increasingly deterministic behavior. The KL-divergence between the approximate posterior and the prior in the complexity term can be written analytically as:

$$\begin{aligned} D_{KL}[q_\phi||p_{\theta_z}] = & \log \frac{\boldsymbol{\sigma}^{p,l}}{\boldsymbol{\sigma}^{q,l}} \\ & + \frac{(\boldsymbol{\sigma}^{p,l} - \boldsymbol{\mu}_t^{q,l})^2 + (\boldsymbol{\sigma}^{q,l})^2}{2(\boldsymbol{\sigma}^{p,l})^2} - \frac{1}{2} \end{aligned} \tag{10}$$

In the posterior inference, all learning-related network parameters of θ and ϕ and the posterior latent variable parameterized by the adaptive variable $\mathbf{A}$ are updated to maximize the lower bound, as shown in Eq. (9), by back-propagating the error from time step T back to t_0 [30].

3) PV-RNN in Dyadic Robot Interaction: Two robots equipped with the PV-RNN model interact during a task of synchronized imitation. In the interaction, the robots predict proprioception $\mathbf{X}_{t+1}^{pr}$ and exteroception $\mathbf{X}_{t+1}^{ex}$ for the next time step. The predicted $\mathbf{X}_{t+1}^{pr}$ regulates joint angle movements of a robot by considering a PID controller. This movement can be sensed by the other robot in terms of exteroception $\bar{\mathbf{X}}_{t+1}^{ex}$ that is provided through the kinematic transformation of joint angles $\mathbf{X}_{t+1}^{pr}$ (see Fig. 2).

Note that while in the training phase, the error signal is taken from the proprioceptive $\bar{\mathbf{X}}^{pr}$ as well as the exteroceptive $\bar{\mathbf{X}}^{ex}$ target sequences in the interaction phase. The error signal for each robot is taken only from exteroception

[1]Setting $\mathbf{w}_1^l = 1$ imposes a unit Gaussian prior at time step $t = 1$. This design is not intended to decrease the initial sensitivity of the network to specific target sequences, but rather to make it more adaptable.

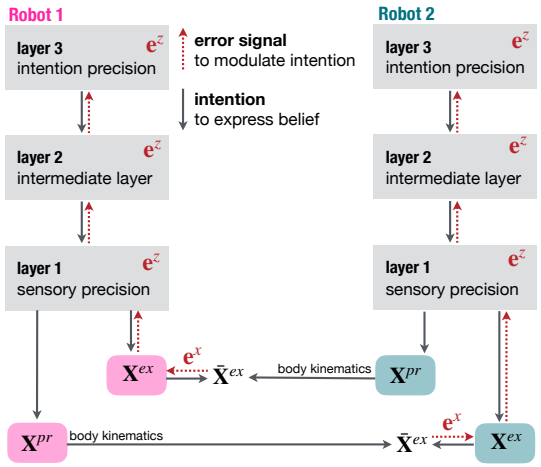

Fig. 2: **Schematic of dyadic robot interaction.**

$\bar{\mathbf{X}}^{ex}$[2]. Prediction errors $\mathbf{e}^x$ are generated and propagated bottom-up throughout all layers, as well as time steps in the posterior inference window, in terms of the latent error $\mathbf{e}^z$. This updates posterior distributions in the network and minimizes the variational free energy. Now, only $\mathbf{A}_{0:T}$ is updated without updating network learning parameters.

III. Robot Experiments

To investigate how the interaction of two robots changes with tighter and looser regulation of complexity, we used an imitative interaction task [17]. First, each robot was trained and tested individually, as described in III-B and in III-C, respectively. Finally, these two robots were examined during a dyadic interaction (III-D).

A. Task Design

Robotic agents are trained with probabilistic sequences consisting of three different movement primitives, A, B, and C (Fig. 3 (a)). Movement primitives are combined to form a continuous pattern that follows a probabilistic sequence. Two probabilistic patterns were trained, A20%B80%C and A80%B20%C as shown in the form of a probabilistic finite state machine (P-FSM) (Fig. 3 (c)). The difference between these two probabilistic patterns is that C comes more often (80%) than B (20%) after A in the former, and vice versa for the latter.

A point of interest is the interaction phase after the learning phase. Although it is expected that both robots can generate A synchronously, since it is a deterministic state, this could be different than generating B or C as two robots learned different preferences in terms of transition probabilities. One robot may lead so as to generate B or C while the other may just follow it. However, both robots may generate their own intended movement preferences by ignoring each other. The current study hypothesizes that whether B or C is generated synchronized or desynchronized between the two robots should depend on complexity regulation of each robot.

[2]This approach assumes that the PID controller generates only negligible position errors for the joints.

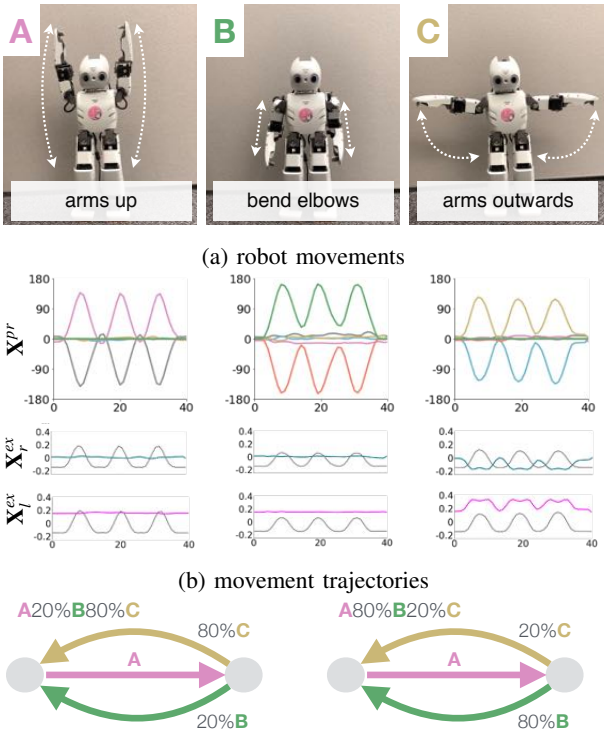

(a) robot movements

(b) movement trajectories

(c) probabilistic transition

Fig. 3: **Task design.** Robot movement primitives A, B, and C of the training dataset (a). Proprioceptive trajectories $\mathbf{X}^{pr}$ and exteroceptive trajectories $\mathbf{X}_r^{ex}$ and $\mathbf{X}_l^{ex}$ for the xy-coordinates of the right and left end effector (b). Two P-FSMs representing different movement primitive transition patterns of A20%B80%C and A80%B20%C (c).

B. Robot Training

Training data for each robot was generated via a master control of a humanoid OP2[3] by a human experimenter, considering the own body mirroring condition. More specifically, while the proprioceptive trajectory $\mathbf{X}^{pr}$ is generated, the exteroceptive trajectory $\mathbf{X}^{ex}$ is also generated by mirroring the own movement using the kinematic transformation (Fig. 3b). $\mathbf{X}^{pr}$ and $\mathbf{X}^{ex}$ are six and four dimensions, respectively. Training data consisted of 20 samples, in which each sample had ten dimensions with 400 time steps.

The PV-RNN was trained with a set of different parameters (TABLE I). Each parameter setting was repeated with different random seeds to ensure reproducibility. Networks

TABLE I: **Network Parameters**

	$\mathbf{d}$	$\mathbf{z}$	τ	$\mathbf{w}_1$	$\mathbf{w}_{2:T}$
layer 1	40	4	2	1	$\mathbf{w}^1 = [0.0, 0.001, ...4.999, 5.0]$
layer 2	20	2	4	1	$\mathbf{w}^2 = w^1 \times 10$
layer 3	10	1	8	1	$\mathbf{w}^3 = w^1 \times 100$

were trained for 80,000 epochs, using Adam Optimizing and back-propagation through time (BPTT) [30] with learning

[3]Humanoid OP2 and its master controller are developed by Robotis: www.robotis.us/robotis-op2-us/

rate 0.001. After training, network performance was first analysed in stand-alone robot experiments (subsection III-C). Thereafter, dyadic robot interaction was studied using networks trained with $\mathbf{w}$ set for the two extremes of tight and loose regulation of FEP complexity (subsection III-D).

C. Stand Alone Robot Experiments

To investigate how the model learns the probabilistic structure of the training data, we conducted a first analysis in the form of *prior regeneration*. *Prior regeneration* uses two time steps of the adaption variable $\mathbf{A}^{\bar{\mathbf{X}}}_{1:2}$ of one selected training sample. $\mathbf{A}^{\bar{\mathbf{X}}}_{1:2}$ initializes the prior distribution $p(\mathbf{z}_{1:2})$ in the PV-RNN to generate the future prediction $\mathbf{X}_{3:400}$ for the remaining training sample length (cf. *prior generation* in Fig. 1). Using this scheme, we generated 20 sequences for each meta-prior $\mathbf{w}$ and all random seeds trained for that parameter. For brevity, training analysis is reported only for the network that was trained on the probabilistic sequence A20%B80%C. Training of A80%B20%C showed comparable results. An Echo State Network for multivariate time series classification [31] with reservoir size $N = 45$, 25% connectivity and leakage 60% was used for classification of movement primitives in the performance analysis and interaction experiments. Movement patterns were classified as *not identified* below a 55% threshold.

1) Analysis of Probabilistic Transition: Let us consider for now, that each network is trained with A20%B80%C. This means that after a robot generates A movement, it will transition to B with 20 percent probability and to C with 80 percentage probability. We found that smaller $\mathbf{w}$ settings are not stable in reproducing the probabilistic structure of the training data. The BC-ratio was either greater or less than 20% for B or greater or less than 80% for C respectively. Networks trained with larger meta-priors become more reliable in regenerating the probabilistic training sequence (cf. BC-ratio in Table II). In addition to the capacity of learning the probability distribution of the training data, we found that smaller meta-priors show noisier pattern generation compared to networks trained with larger $\mathbf{w}$'s. Non-classified movements were as high as $22\% \pm 4$ with $\mathbf{w} = 0.01$ and decreased to $6\% \pm 0.6$ with $\mathbf{w} = 3.4$.

2) Divergence Analysis: Repeatability in generating sequences in prior generation was examined by conducting a divergence analysis. Sequences are considered diverged when a comparison per time step of $\mathbf{X}^{pr}$ exceeds a threshold[4]. Out of 20 regeneration sequences, we randomly select one as a reference and calculate the average divergence step of the other sequences to this the reference. Out of 400 time steps of prior generation, sequences diverged from the reference around time step 43 for networks trained with smaller $\mathbf{w}$. With increasing $\mathbf{w}$, repeatability of the trajectories increased, as also indicated in [21]. Here the divergence step was around 139 (cf. divergence step t in Table II).

[4]We use the mean squared error of joint angle data $[-180, 180]$ of $\mathbf{X}^{pr}$. The threshold is set to 50.

3) Summary of Stand-Alone Robot Experiments: Loose regulation of the complexity term results in noisier, less repeatable prior generation performance, resulting in more stochastic dynamics. Also the learned probability for transition to either B or C is not accurate. This observation changes with increasing meta-prior. The larger $\mathbf{w}$, the more accurate the learned transition probability becomes. Also, prior generation becomes more repeatable, which means that increasingly deterministic dynamics are developed. For subsequent dyadic robot interaction experiments, we empirically select the meta-prior setting $\mathbf{w} = 0.005$ and $\mathbf{w} = 3.4$ to represent two extremes of tighter and weaker regulation of the FEP complexity.

D. Dyadic Robot Interaction Experiments

1) Experiment Setup: In the following experiments, robots are either trained with $\mathbf{w} = 0.005$ or $\mathbf{w} = 3.4$. For readability, instead of referring to the two interacting robots with their parameter settings, we will consider $\mathbf{R}^1_w$ and $\mathbf{R}^2_w$ with subscripts of the respective meta-priors $\mathbf{w}$. In the dyadic interaction, we present the network of each robot with observations of movements of the counterpart robot $\bar{\mathbf{X}}^{ex}$ as the target and perform posterior inference in a limited regression window with size $win_{size} = 70$. Inference is performed from the current time step t back to $t - win_{size}$, or t_0 in case $t - win_{size} \leq 0$ (cf. Fig. 1, where posterior inference is carried out from time step 2 to time step 3). After 200 epochs of iteration to maximize the lower bound, the time window is shifted one time step forward. Note, all experiments were conducted in simulation due to the difficulty of real-time posterior inference computation.

We investigated how two robots interact in three different dyadic conditions (TABLE III). We then analysed whether the robots trained with A80%B20%C maintained the learned preference between B and C or adapted to their counterparts that were trained with A20%B80%C. We also calculated the so-called BC-synchronization rate during the interaction. When at any time step t, one of the robots generated B or C and the other robot generated the same movement primitive, the interaction was considered synchronized. The BC-synchronization rate is the ratio of synchronization computed in this way averaged over all time steps. Note that time steps in which movement patterns generated were identified as *not classified* by the Echo State Network were excluded from the computation.

TABLE III shows the summary of the analysis for all three experiments. To better understand effects of loose and tight regulation of FEP complexity, exemplar plots of robot movement patterns, as well as corresponding network dynamics, are shown (see Fig. 4 and Fig. 5). We provide supplementary movies of the experiments showing humanoid robot interaction and network dynamics here: https://figshare.com/s/77d059634ef4f062e332.

2) Experiment 1: $\mathbf{R}^1_{0.005}$ vs. $\mathbf{R}^2_{3.4}$: In Experiment 1, $\mathbf{R}^1_{0.005}$ adapts to the probabilistic transition of $\mathbf{R}^2_{3.4}$ by increasing the probability of transition to B from 22% in the stand alone condition to 86% in the dyad (Table III

TABLE II: **Training performance** of representative meta-prior $\mathbf{w}$. The mean and standard deviation represent three random seeds and 20 repetitions of prior generation for each $\mathbf{w}$.

$\mathbf{w}$	training sequence A20%B80%C				BC-ratio	divergence step t
	A	B	C	not classified		
0.005	34 ± 1	11 ± 3	40 ± 2	15 ± 1	22 ± 6B 78 ± 5C	43
0.01	35 ± 2	13 ± 0.2	30 ± 2	22 ± 4	30 ± 5B 70 ± 5C	50
1.0	36 ± 1	11 ± 2	40 ± 2	13 ± 0.2	22 ± 4B 78 ± 4C	91
2	41 ± 0.7	10 ± 0.5	39 ± 0.7	10 ± 0.3	21 ± 8B 79 ± 8C	120
3.4	45 ± 1	11 ± 1	38 ± 2	6 ± 0.5	24 ± 2B 76 ± 2C	139

TABLE III: **Interaction performance** of three experimental settings.

Experiment		BC-ratio				BC-sync
ID	robots	stand alone		interaction		
		B	C	B	C	
1	$\mathbf{R}^1_{0.005}$ $\mathbf{R}^2_{3.4}$	22 ± 6 75 ± 2	78 ± 5 25 ± 3	86 ± 6 92 ± 8	14 ± 5 8 ± 6	57 ± 18
2	$\mathbf{R}^1_{3.4}$ $\mathbf{R}^2_{3.4}$	24 ± 2 74 ± 2	76 ± 2 25 ± 3	13 ± 6 81 ± 8	87 ± 13 19 ± 9	29 ± 16
3	$\mathbf{R}^1_{0.005}$ $\mathbf{R}^2_{0.005}$	22 ± 6 44 ± 11	78 ± 5 56 ± 11	68 ± 15 36 ± 9	32 ± 10 64 ± 13	29 ± 18

Experiment 1). Both robots are performing more B than C with a BC synchronization rate of 57%.

Fig. 5 shows an example of how prediction of the future and posterior inference of the past proceed as time passes from time step 200, 230, to 260 for both robots. We observe that the intended future behavior (the prior generation) of $\mathbf{R}^1_{0.005}$ is not consistent with the actually performed actions after posterior inference. On the other hand, in the case of $\mathbf{R}^2_{3.4}$, the performed action complies with its prediction. This observation can be explained by looking at the difference of discrepancies between exemplar priors μ^p and posteriors μ^q between two robots shown in Fig. 4a. Discrepancies between μ_1^{1q} and μ_1^{1p} as well as μ_2^{1q} and μ_2^{1p} in layer 1 of $\mathbf{R}^1_{0.005}$ are larger than those of $\mathbf{R}^2_{3.4}$. More specifically, the average KL-divergence of $\mathbf{R}^1_{0.005}$ is much larger for all layers $((\mathbf{e}^{z,1}, \mathbf{e}^{z,2}, \mathbf{e}^{z,3}) = (109.1, 1.4, 0.06))$ than for $\mathbf{R}^2_{3.4}$ $((\mathbf{e}^{z,1}, \mathbf{e}^{z,2}, \mathbf{e}^{z,3}) = (0.4, 0.0003, 0.00001))$. This means that $\mathbf{R}^2_{3.4}$ tends to behave as intended because the posterior is attracted by the prior with the stronger constraint of minimizing the KL-divergence. Here, the belief is stronger than the observation. On the other hand, $\mathbf{R}^1_{0.005}$ tends to adapt to $\mathbf{R}^2_{3.4}$ since the posterior is attracted more by the observation than by the weaker prior belief. Note that μ_1^{3q} and μ_1^{3p} in layer 3 change only slowly with time. This indicates that these latent variables represent how movement primitives transit from deterministic states to non-deterministic states using their slower timescale properties.

3) Experiment 2: $\mathbf{R}^1_{3.4}$ vs. $\mathbf{R}^2_{3.4}$: When two robots with loose complexity regulation interact, both robots maintain their learned probability preferences in generating B or C. $\mathbf{R}^1_{3.4}$, which learns a 76% transition to C in a stand-alone situation, shows its preference to C in the dyad with probability of 87%. $\mathbf{R}^2_{3.4}$, which in a stand-alone condition would maintain its preference to B with a probability of 74%, shows 81% percentage transition to B in the interaction. BC-synchronization rate turns out to be 29%. This means that two robots mostly do not imitate each other when generating B or C. By examining network dynamics of the prior and posterior distributions, the robots seem to follow their intentions, i.e. they execute movements based upon their predictions without adapting their own posteriors to observations of the other robot's movement (cf. Fig. 4b).

4) Experiment 3: $\mathbf{R}^1_{0.005}$ vs. $\mathbf{R}^2_{0.005}$: When two agents with tight regulation of complexity interact, both try to adapt their own behavior to the actions of the other. Whether trained on a A20%B80%C or a A80%B20%C probabilistic transition, robots significantly reduce the tendency to perform their own intended behavior C or B, respectively. This is evidenced by changes of the BC-ratio from stand-alone compared to the dyadic setting (TABLE III Experiment 3). The interaction becomes noisier, compared to results of Experiments 1 and 2 (Fig. 4c), which indicate that tight regulation makes robots more sensitive to temporal fluctuations in observations of their counterparts. As in Experiment 2, the probabilistic transition is synchronized only in 29% (TABLE III Experiment 3). This is due to the fact that neural dynamics of each robot become too stochastic to synchronize because of the tight complexity regulation. Indeed, Fig. 4c shows that the prior and posterior do not comply, but deviate.

5) Summary of Dyadic Robot Experiments: We observed that the type of dyadic interaction varies depending on the tightness of regulation of the complexity term controlled by the value of meta prior w. When one robot trained with tighter regulation and another trained with looser regulation interact, the latter tends to lead the interaction by exerting stronger prior intention, while the former tends to follow by adapting its own posterior to its observations. When both robots are trained with looser regulation of complexity, each of them tends to generate its own intended movements without adapting to the other. This is because in both robots, the posterior is drawn more strongly by the prior than the observation. Finally, when both robots are trained with tighter complexity regulation, each tends to generate more stochastic movement patterns with weaker prior intention. This causes more fluctuation in the dyadic interaction.

IV. Discussion

The current study examines how social interaction in robotic agents dynamically changes depending on the sense of agency (SoA) of each individual. For this purpose, we conducted simulation experiments on dyadic imitative in-

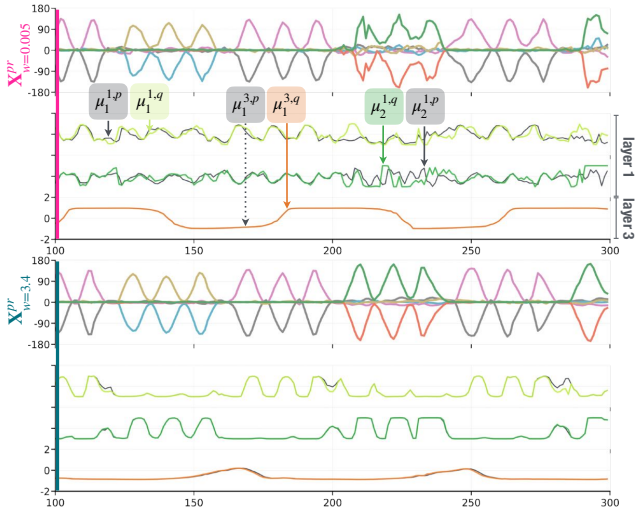

(a) Experiment 1: $\mathbf{R}^1_{0.005}$ vs $\mathbf{R}^2_{3.4}$

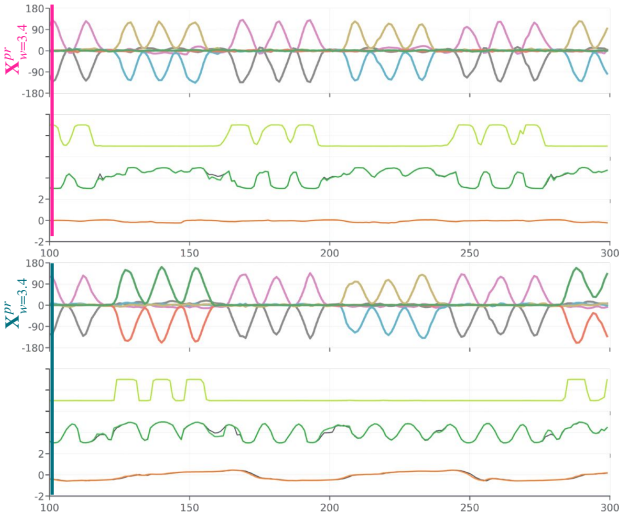

(b) Experiment 2: $\mathbf{R}^1_{3.4}$ vs $\mathbf{R}^2_{3.4}$

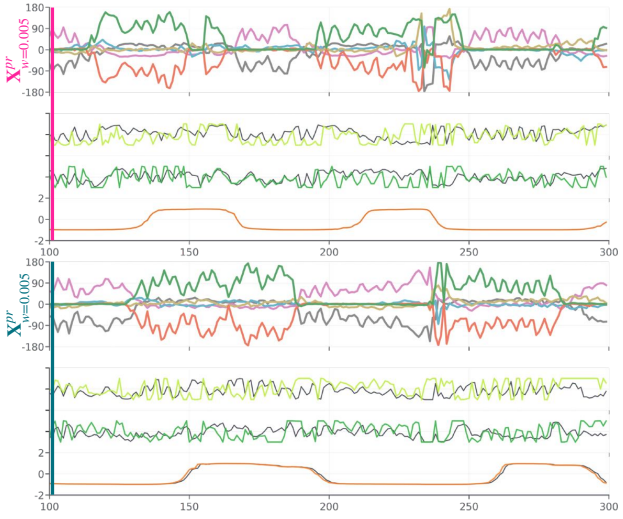

(c) Experiment 3: $\mathbf{R}^1_{0.005}$ vs $\mathbf{R}^2_{0.005}$

Fig. 4: **Movement trajectories and network dynamics of dyadic robot interaction** for Experiment 1 (a), Experiment 2 (b) and Experiment 3 (c). Time steps $t = [100, 300]$ of movements and selected neurons in layer 1 and 3 are shown.

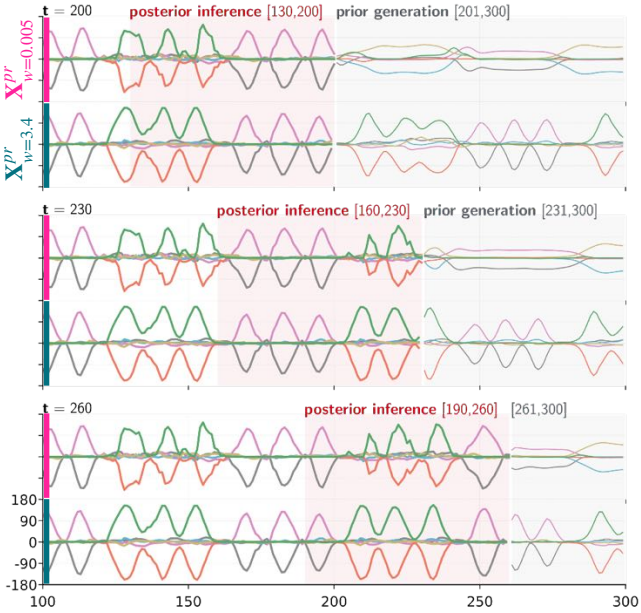

Fig. 5: **Posterior inference and prior generation in Experiment 1**. Interaction of $\mathbf{R}^1_{0.005}$ (upper) and $\mathbf{R}^2_{3.4}$ (lower) in terms of $\mathbf{X}^{pr}$. The first, the second, and the third row show $\mathbf{X}^{pr}$ after the posterior inference in the inference window with size $win_{size} = 70$, as well as its future prior generation with current time steps of 200, 230, and 260, respectively.

teractions by humanoids equipped with PV-RNN architectures. PV-RNN is a hierarchically organized variational RNN model that employs a framework of predictive coding and active inference based on the free energy principle.

The PV-RNNs with which the robots were equipped were trained in stand-alone conditions by varying the tightness of regulation of the FEP complexity term. We show that PV-RNNs trained with looser regulation of complexity developed stronger SoAs by self-organizing more deterministic dynamics. On the other hand, PV-RNNs trained with tighter regulation of complexity developed weaker SoAs by self-organizing more stochastic dynamics.

Simulation experiments on dyadic imitative interaction revealed different types of interactions between robots depending on different combinations of networks trained with tighter or looser regulation. In the experiment in which a robot with tighter regulation interacts with a robot having looser regulation, the latter tends to lead the interaction by exerting a stronger SoA, while the former tends to follow the latter by adapting its own posterior to its observations. In this setting, the synchronization rate between the two robots was higher than in other settings. When two robots with looser regulation, i.e. stronger SoAs, interact, each tends to generate its own intended movements without adapting to the other. Finally, in a case in which both robots have tighter regulation, a more fluctuating dyadic interaction develops because each tends to generate more stochastic movement patterns as a result of a weaker SoA. Here, we argue that observation in dyadic robot experiments should have instan-

tiated the concept of primary intersubjectivity [28] wherein the cognitive processes of predicting and inferring intentions of others emerge solely through dynamic interaction rather than through deliberative computations.

The current experiments consider a fixed meta-prior setting only. Since the meta-prior is the essential network component to guide SoAs in the proposed framework, future studies should target meta-learning of the meta-prior in developmental processes or through autonomous adaption within dyadic contexts. This could provide further understanding of more complex social interaction phenomena, including turn-taking in the context of adaptive regulation of free energy. Another limitation of the current work is that only synchronized imitation is considered social cognitive behavior. Subsequent work should examine how different types of social interactions are generated spontaneously in different social contexts under the FEP. Synthetic robotic experiments on these issues, in particular with real-time computation, which is expected to develop in the future, should contribute to deeper understanding of social cognitive mechanisms of robots, as well as humans.

REFERENCES

[1] S. Gallagher, "Philosophical conceptions of the self: implications for cognitive science," *Trends in cognitive sciences*, vol. 4, no. 1, pp. 14–21, 2000.

[2] Y. Kuniyoshi, M. Inaba, and H. Inoue, "Learning by watching: extracting reusable task knowledge from visual observation of human performance," *IEEE Transactions on Robotics and Automation*, vol. 10, no. 6, pp. 799–822, 1994.

[3] G. Hayes and Y. Demiris, "A robot controller using learning by imitation," *Citeseer*, vol. 676, 06 1995.

[4] K. Dautenhahn, "Getting to know each other - artificial social intelligence for autonomous robots." *Robotics and Autonomous System*, vol. 16, no. 2-4, pp. 333–356, 1995.

[5] P. Gaussier, S. Moga, M. Quoy, and J. P. Banquet, "From perception-action loops to imitation processes: A bottom-up approach of learning by imitation," *Applied Artificial Intelligence*, vol. 12, no. 7-8, pp. 701–727, 1998.

[6] C. Breazeal and B. Scassellati, "A context-dependent attention system for a social robot," in *Proceedings of the 16th International Joint Conference on Artificial Intelligence - Volume 2*, ser. IJCAI'99. San Francisco, CA, USA: Morgan Kaufmann Publishers Inc., 1999, p. 1146–1151.

[7] G. Di Pellegrino, L. Fadiga, L. Fogassi, V. Gallese, and G. Rizzolatti, "Understanding motor events: a neurophysiological study," *Experimental brain research*, vol. 91, no. 1, pp. 176–180, 1992.

[8] M. Arbib, "The mirror system, imitation, and the evolution of language." *Imitation in animals and artefacts*, pp. 229–280, 2002.

[9] E. Oztop, M. Kawato, and M. Arbib, "Mirror neurons and imitation: A computationally guided review," *Neural networks*, vol. 19, no. 3, pp. 254–271, 2006.

[10] T. Inamura, Y. Nakamura, H. Ezaki, and I. Toshima, "Imitation and primitive symbol acquisition of humanoids by the integrated mimesis loop," in *Proceedings 2001 ICRA. IEEE International Conference on Robotics and Automation (Cat. No.01CH37164)*, vol. 4, 2001, pp. 4208–4213.

[11] A. Billard and M. Mataric, "Learning human arm movements by imitation: Evaluation of a biologically-inspired connectionist architecture," *Robotics and Autonomous Systems*, vol. 941, pp. 1–16, 2001.

[12] E. Oztop, T. Chaminade, G. Cheng, and M. Kawato, "Imitation bootstrapping: experiments on a robotic hand," in *5th IEEE-RAS International Conference on Humanoid Robots, 2005.*, 2005, pp. 189–195.

[13] M. Ito and J. Tani, "On-line imitative interaction with a humanoid robot using a dynamic neural network model of a mirror system," *Adaptive Behavior*, vol. 12, no. 2, pp. 93–115, 2004.

[14] Y. N. Takato Horii and M. Asada, "Imitation of human expressions based on emotion estimation by mental simulation." *Journal of Behavioral Robotics*, vol. 7, pp. 40–54, 2016.

[15] J. Hwang, J. Kim, A. Ahmadi, M. Choi, and J. Tani, "Dealing with large-scale spatio-temporal patterns in imitative interaction between a robot and a human by using the predictive coding framework," *IEEE Transactions on Systems, Man, and Cybernetics: Systems*, vol. 50, no. 5, pp. 1918–1931, 2020.

[16] E. Ugur, Y. Nagai, E. Sahin, and E. Oztop, "Staged development of robot skills: Behavior formation, affordance learning and imitation with motionese," *IEEE Transactions on Autonomous Mental Development*, vol. 7, no. 2, pp. 119–139, 2015.

[17] W. Ohata and J. Tani, "Investigation of the sense of agency in social cognition, based on frameworks of predictive coding and active inference: A simulation study on multimodal imitative interaction," *Frontiers in Neurorobotics*, vol. 14, p. 61, 2020.

[18] K. Friston, "A theory of cortical responses," *Philosophical transactions of the Royal Society B: Biological sciences*, vol. 360, no. 1456, pp. 815–836, 2005.

[19] A. Clark, *Surfing uncertainty: Prediction, action, and the embodied mind*. Oxford University Press, 2015.

[20] K. Friston, "Prediction, perception and agency," *International Journal of Psychophysiology*, vol. 83, no. 2, pp. 248–252, 2012.

[21] A. Ahmadi and J. Tani, "A novel predictive-coding-inspired variational rnn model for online prediction and recognition," *Neural computation*, vol. 31, no. 11, pp. 2025–2074, 2019.

[22] S. Murata, Y. Yamashita, H. Arie, T. Ogata, S. Sugano, and J. Tani, "Learning to perceive the world as probabilistic or deterministic via interaction with others: A neuro-robotics experiment," *IEEE Transactions on Neural Networks and Learning Systems*, vol. 28, no. 4, pp. 830–848, 2017.

[23] P. Lanillos and G. Cheng, "Adaptive robot body learning and estimation through predictive coding," *CoRR*, vol. abs/1805.03104, 2018. [Online]. Available: http://arxiv.org/abs/1805.03104

[24] C. Lang, G. Schillaci, and V. Hafner, "A deep convolutional neural network model for sense of agency and object permanence in robots," *2018 Joint IEEE 8th International Conference on Development and Learning and Epigenetic Robotics (ICDL-EpiRob)*, pp. 257–262, 2018.

[25] D. Oliva, A. Philippsen, and Y. Nagai, "How development in the bayesian brain facilitates learning," in *2019 Joint IEEE 9th International Conference on Development and Learning and Epigenetic Robotics (ICDL-EpiRob)*, 2019, pp. 1–7.

[26] Y. Yamashita and J. Tani, "Emergence of functional hierarchy in a multiple timescale neural network model: a humanoid robot experiment," *PLoS computational biology*, vol. 4, no. 11, p. e1000220, 2008.

[27] H. F. Chame, A. Ahmadi, and J. Tani, "A hybrid human-neurorobotics approach to primary intersubjectivity via active inference," *Frontiers in Psychology*, vol. 11, p. 3207, 2020.

[28] C. Trevarthen, "Communication and cooperation in early infancy: A description of primary intersubjectivity," *Before speech: The beginning of interpersonal communication*, vol. 1, pp. 530–571, 1979.

[29] J. Chung, K. Kastner, L. Dinh, K. Goel, A. C. Courville, and Y. Bengio, "A recurrent latent variable model for sequential data," in *Advances in neural information processing systems*, 2015, pp. 2980–2988.

[30] D. E. Rumelhart, G. E. Hinton, and R. J. Williams, "Learning internal representations by error propagation," California Univ San Diego La Jolla Inst for Cognitive Science, Tech. Rep., 1985.

[31] F. M. Bianchi, S. Scardapane, S. Løkse, and R. Jenssen, "Reservoir computing approaches for representation and classification of multivariate time series," *IEEE transactions on neural networks and learning systems*, vol. PP, 2020.